Desalination and Water Treatment
www.deswater.com
doi: 10.1080/19443994.2014.941308

56 (2015) 695–708
October

Taylor & Francis
Taylor & Francis Group

Removal of a reactive textile azo dye by dolomitic solids: kinetic, equilibrium, thermodynamic, and FTIR studies

Samira Ziane[a], Kheira Marouf-Khelifa[a], Houari Benmekki[b], Jacques Schott[c], Amine Khelifa[a,*]

[a]*Laboratoire de Structure, Elaboration et Applications des Matériaux Moléculaires (S.E.A.2M.), Département de Chimie, Université de Mostaganem, B.P. 981, R.P., Mostaganem 27000, Algeria, Tel. +213 45 21 60 80; Fax: +213 45 21 10 18; email: aminekhelifadz@yahoo.fr (A. Khelifa)*
[b]*Faculté des Sciences Exactes et Informatique, Université de Mostaganem, Mostaganem 27000, Algeria*
[c]*Laboratoire Géosciences Environnement Toulouse (GET), CNRS-IRD-OMP-Université de Toulouse, 14, Avenue Edouard Belin, 31400 Toulouse, France*

Received 11 February 2014; Accepted 26 June 2014

ABSTRACT

Algerian dolomite was treated at different temperatures in the 600–1000°C range and characterized by XRD and SEM. The obtained samples, named dolomitic solids, were used in the removal of Reactive Black 5 (RB5) from aqueous solutions. A literature survey shows that the data about the dye adsorption by dolomites are almost non-existent. Kinetic data, equilibrium isotherms, thermodynamic parameters, pH influence, and FTIR study were considered. The kinetic mechanism is enough complex, involving different models such as those of pseudo-second-order, intraparticle diffusion, and Elovich. For all dolomitic solids, the capacity in RB5, at equilibrium, strongly increases with increasing adsorption temperature. The affinity sequence is D900 (dolomite treated at 900°C) > D800 > D1000 > D600 > raw dolomite. Knowing that D900 adsorbs 125.9 mg g^{-1}, it appears very effective for removing reactive dyes from wastewaters. The isotherms are found to be overall well represented by the Redlich–Peterson equation. The fact that maximum adsorption occurs at isoelectric point emphasizes the prevalence of the nonelectrostatic interaction. A close agreement exists between the evolution of kinetic, equilibrium, and thermodynamic parameters, suggesting chemisorption. The process reflects for D800, D900, and D1000 a weak chemical interaction via a mechanism of inner-sphere complexation. The comprehension of the organic compound–dolomitic solid interactions constitutes a fundamental aspect for developing the application of these materials in the field of wastewater treatment.

Keywords: Dolomite; Reactive Black 5; Removal; Kinetics; Isotherms; Mechanism

1. Introduction

Synthetic dyes are widely used in textile, paper, rubber, plastic, leather, cosmetic, pharmaceutical, and food industries. They are classified into three categories: (1) anionic: acid, direct, and reactive dyes; (2) cationic: basic dyes; and (3) non-ionic: disperse dyes [1]. The reactive dyes are most used, due to their advantages such as bright colors, excellent colorfastness, and ease of application [2]. They are representing 20–30%

*Corresponding author.

of the dye market and are widely used in the textile industry [3]. After use, they are generally released into effluents. Their presence in wastewaters generates huge problems for the environment and living organisms because they are recalcitrant organic molecules, resistant to aerobic digestion, stable to light, heat, and oxidizing agents [4]. Color is the first contaminant to be recognized in wastewater. The presence of very small amounts of dyes in water is highly discernible and undesirable [5]. Furthermore, the expanded uses of dyes showed that some of them and their reaction products, such as aromatic amines, are highly carcinogenic.

C.I. Reactive Black 5 (RB5) was chosen in this study because it is extensively used in textile industry. It develops a covalent bonding with textile fibers such as cotton via reactive groups [5]. After use, different techniques have been used to treat this contaminant: biological treatment [6], mineralization [7], photocatalytic decolorization [8], and nanofiltration [9]. These techniques suffer from a certain number of problems such as high cost, not effective for all dyes and optimization of the operational parameters. Adsorption was found to be an effective, economical, and easy technique to implement. Its other advantages are applicability at very low concentrations, uses in batch and continuous processes, little sludge generation, and possibility of regeneration and reuse.

Dolomite is an important industrial mineral. Its structure contains alternating planes of Ca^{2+} and Mg^{2+} cations, with an ideal formula of $CaMg(CO_3)_2$. A literature survey shows that there are several articles dedicated to its applications in the field of refractories and catalysts [10–12]. On the contrary, there is no paper dealing with the study of the mechanisms and characteristics of retention of dyes by dolomites, so that the removal of C.I. RB5 by Algerian dolomite and its calcined derivatives becomes pertinent.

The objective of this work is to examine the possibility of using this material for the RB5 removal from aqueous solutions. Before adsorption experiments, Algerian dolomite was treated at different temperatures in the 600–1,000°C range and characterized by XRD and SEM. The effects of solution concentration, contact time, temperature, and pH have been evaluated. A particular attention has been focused on the mechanism of RB5 retention.

2. Materials and methods

2.1. Materials

Raw dolomite from Ouled Mimoun, Tlemcen (Western region of Algeria) was used in this work. The grain size was 0.125–0.25 mm. Samples of raw dolomite were heated in a muffle furnace at 600, 800, 900, and 1000°C. Each sample was processed at the relevant temperature for 2 h. It is well known that 2 h is a sufficient time so that heat penetrates until the interior of the particles and induces some transformations, for a certain number of materials [13–15]. The samples were named dolomite, D600, D800, D900, and D1000. The partial decomposition of dolomite carried out in the 600–1000°C range provided new adsorbents called dolomitic solids.

2.2. Characterization

The chemical composition of dolomite was determined by a Cameca SX-50 electronic microprobe and is: 31.18% CaO, 21.05% MgO, 0.02% Fe_2O_3, 0.01% SiO_2, 0.002% Al_2O_3, 0.0015% MnO_2, and 0.01% Cr_2O_3. X-ray powder diffraction patterns were obtained using a Philips PW 1830 diffractometer with CoK_α radiation ($\lambda = 0.1789$ nm). The XRD data were collected over a 2θ range of 5°–110°. The crystallite size and morphology of the samples were determined by scanning electronic microscopy (JEOL, JSM-6360, Japan). The IR spectra were recorded on a Shimadzu Prestige 21 spectrophotometer using a pellet (pressed-disk) technique. For this, the adsorbent was intimately mixed with approximately 100 mg of dry powdered KBr.

2.3. Adsorption procedure

C.I. RB5 (CAS No: 17095-24-8, chemical formula $C_{26}H_{21}O_{19}N_5S_6Na_4$, FW: 991.8 g/mol, λ_{max}: 597 nm), a commercial diazo reactive dye containing two vinyl sulfone as reactive groups (Fig. 1), was supplied by Sigma–Aldrich, Germany.

The working solutions of RB5 were prepared by diluting a stock solution of concentration 1 g L^{-1} into

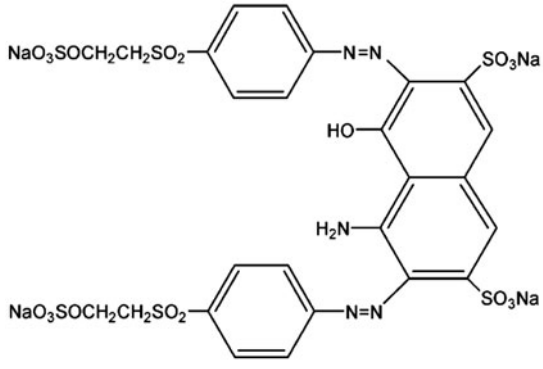

Fig. 1. Chemical structure of RB5.

the desired concentrations. The adsorption experiments were performed via the batch method. 0.02 g of dolomitic solid was mixed with 20 mL of aqueous RB5 solution. After each experiment, the solution was separated by centrifugation. The supernatant was analyzed by visible spectrophotometry, at 597 nm, using a Shimadzu 1240 UV–vis spectrophotometer. The adsorbed amount was calculated from the difference between the initial and final concentrations. The effects of contact time, concentration, temperature, and pH were studied. The experimental conditions are outlined in Table 1.

2.4. Theoretical considerations

2.4.1. Adsorption kinetics

In order to investigate the controlling mechanism of the adsorption process, various kinetic equations were applied to test the experimental data. Lagergren [16] proposed a pseudo-first-order kinetic model. The integral form of the model is

$$\log(Q_e - Q_t) = \log Q_e - \frac{K_1 t}{2.303} \quad (1)$$

where Q_t is the amount adsorbed at time t (mg g^{-1}), Q_e the adsorption capacity at equilibrium (mg g^{-1}), K_1 the pseudo-first-order rate constant (min^{-1}), and t is the contact time (min).

The adsorption kinetics may also be described by a pseudo-second-order reaction. The linearized-integral form of the model is [17]:

$$\frac{t}{Q_t} = \frac{1}{K_2 Q_e^2} + \frac{t}{Q_e} \quad (2)$$

Table 1
Experimental conditions during the adsorption of RB5

Contact time	1, 3, 5, 10, 20, 40, 60, 120, 240 min; $C_{initial}$ = 80 mg L^{-1} [solid]/[solution]: 1 g L^{-1}; T: 25, 40, 55°C; pH: 6.9
Concentration	20, 40, 60, 80, 100, 150, 200, 300, 400 mg L^{-1} [solid]/[solution]: 1 g L^{-1}; contact time: 2 h; pH: 6.9
Temperature	25, 40 and 55°C, [solid]/[solution]: 1 g L^{-1}; contact time: 2 h; pH: 6.9
pH	pH 3.1–5.0–6.9–9.0–11.0; $C_{initial}$ = 80 mg L^{-1} [solid]/[solution]: 1 g L^{-1}; contact time: 2 h; T: 25°C

where K_2 (g mg^{-1} min^{-1}) is the pseudo-second-order rate constant of adsorption. The initial adsorption rate, h, as $t \to 0$, can be defined as

$$h = K_2 \cdot Q_e^2 \quad (3)$$

The plot of t/Q_t vs. t should give a linear relationship, from which K_2 and h can be determined from the slope and intercept of the plot.

During adsorption under batch mode, there is a possibility of transport of adsorbate species into the pores of adsorbent, which is often the rate controlling step. The intraparticle diffusion rate equation can be written as follows [18]:

$$Q_t = K_{id} t^{1/2} + C \quad (4)$$

where K_{id} (mg g^{-1} min$^{-1/2}$) is the intraparticle diffusion rate constant and C is a constant. The values K_{id} and C are calculated from the slope and the intercept, respectively, of the plot of Q_t vs. $t^{1/2}$.

The Elovich equation is one of the most useful models for describing chemisorption. It is generally expressed as follows [19]:

$$Q_t = \frac{1}{\beta}\ln(\alpha \cdot \beta) + \frac{1}{\beta}\ln t \quad (5)$$

where α is the initial adsorption rate (mg g^{-1} min^{-1}), β is the desorption constant (g mg^{-1}) for Chien–Clayton equation. The parameters α and β can be obtained from the linear plots of Q_t vs. $\ln t$.

2.4.2. Adsorption isotherms modeling

The equilibrium models of Langmuir, Freundlich, Langmuir–Freundlich (LF), and Redlich–Peterson (RP) were used to fit the experimental data. The Langmuir equation can be written under the following form [20]:

$$\frac{C_e}{Q_e} = \frac{1}{Q_m \cdot K_L} + \frac{C_e}{Q_m} \quad (6)$$

where Q_e is the equilibrium amount removed from solution (mg g^{-1}), C_e is the equilibrium concentration (mg L^{-1}), K_L is a constant related to the affinity of binding sites (L mg^{-1}), and Q_m is the maximum amount per unit weight of adsorbent for complete monolayer coverage (mg g^{-1}).

The Freundlich model has been widely adopted and may be written under the form [21]:

$$\log Q_e = \log K_F + \frac{1}{n}\log C_e \tag{7}$$

where K_F is a constant taken as an indicator of adsorption capacity (L g^{-1}) and $1/n$ is a constant indicative of the adsorption intensity.

The three-parameter LF [22] and RP [23] equations have been proposed to improve the fit by the Langmuir or Freundlich equations and are given by Eqs. (3) and (4), respectively:

$$Q_e = \frac{K_{LF}C_e^{\beta}}{1 + a_{LF}C_e^{\beta}} \tag{8}$$

$$Q_e = \frac{K_{RP}C_e}{1 + a_{RP}C_e^{\beta}} \tag{9}$$

where Q_e (mg g^{-1}) is the amount adsorbed at equilibrium, C_e (mg L^{-1}) is the equilibrium solution concentration, K is the equilibrium constant (L mg^{-1}), β is the heterogeneity factor that depends on surface properties of the adsorbent, and M (mg g^{-1}) is the maximum amount adsorbed.

2.4.3. Thermodynamic study

The thermodynamic parameters ΔG, ΔH, and ΔS were evaluated using the equation:

$$\ln K_d = (-\Delta H/R \cdot T) + (\Delta S/R) \tag{10}$$

where ΔH and ΔS are the change in enthalpy (kJ mol^{-1}) and entropy (J mol^{-1} K^{-1}), respectively. T the absolute temperature (K), R gas constant (J mol^{-1} K^{-1}), and K_d is the distribution coefficient (L g^{-1}). This coefficient reflects the overall RB5-surface affinity and is given by:

$$K_d = Q_e/C_e \tag{11}$$

The enthalpy and entropy changes are graphically determined by plotting ln K_d vs. $1/T$, which gives a straight line. According to thermodynamics, the Gibbs free energy change, ΔG, is related to ΔH and ΔS at constant temperature by the following equation:

$$\Delta G = \Delta H - T\Delta S \tag{12}$$

3. Results and discussion

3.1. Modification and characterization

Thermal treatment up to 1,000˚C causes a decomposition of dolomite, which was discussed previously from XRD analysis [24,25]. The identification of the obtained phases is listed in Table 2. The heating of dolomite at 600˚C for 2 h does not modify the structure significantly except the appearance of a minor amount of calcite. According to the literature data [26], the decomposition of dolomite above 700˚C occurs in air in two steps, as follows:

$$\text{first reaction: } CaMg(CO_3)_2 \rightarrow CaCO_3 + MgO + CO_2 \tag{13}$$

$$\text{second reaction: } CaCO_3 \rightarrow CaO + CO_2 \tag{14}$$

The product of partial decomposition corresponding to the first reaction occurs at about 800˚C and leads to calcium carbonate (calcite) and magnesium oxide. The second reaction proceeds from 900˚C. The product consists of a rigid porous calcite and the fine powdered magnesium oxide [27]. Dolomite treated at 1,000˚C undergoes a total decomposition with the formation of an oxide crystal network constituted of lime

Table 2
Thermal treatment parameters and XRD analysis

Sample	Mode of preparation	Mineralogical species	Weight loss %
Raw dolomite	–	Dolomite (D), quartz (Q)	–
D600	Heating for 2 h at 600˚C	Dolomite (D), calcite (C), quartz (Q)	6
D800	Heating for 2 h at 800˚C	Calcite (C), MgO, CaO, quartz (Q)	30
D900	Heating for 2 h at 900˚C	MgO, CaO, calcite (C)	47
D1000	Heating for 2 h at 1,000˚C	MgO, CaO	48

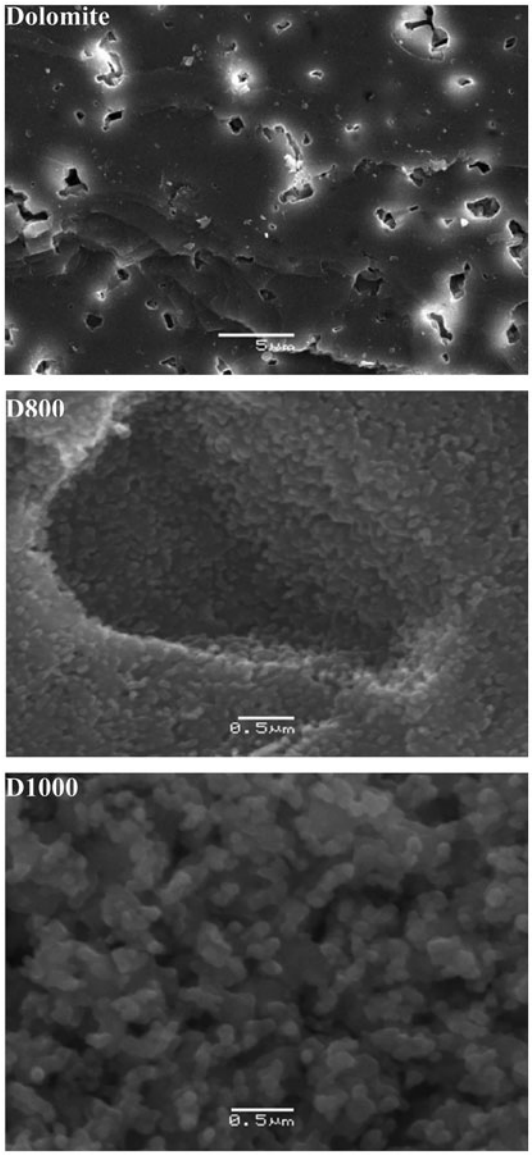

Fig. 2. SEM images of dolomite, D800, and D1000.

and periclase. These considerations explain the choice of 600, 800, 900, and 1,000 °C.

SEM images of dolomite, D800 and D1000 are depicted in Fig. 2. Dolomite evidences a compact structure with presence of bright area due to an inclusion of quartz. After thermal modification, the surface topography is profoundly affected. The micrograph of D800 reveals newly created pores and slots. The structure appears to be less compact than that of the starting material. The image of D1000 shows that the original particle shape is totally destroyed at 1,000 °C, forming small spherical particles with a diameter of 0.1 μm. From 800 °C, the CO_2 release leads to a more porous structure so that the adsorption of RB5 by D800, D900, and D1000 is probably favored.

3.2. Effect of contact time and kinetic study

The effects of contact time and temperature are shown in Fig. 3. From 1 to 10 min, the suspensions were quickly filtered to stop the reaction of adsorption. At 25 °C, it can be seen that the adsorption rate is rapid in the first 20 min, corresponding to the removal of 68% of the RB5 concentration for D800, D900, and D1000 and 41% for dolomite and D600. After this initial stage, the rate gradually decreases, reaching equilibrium at about 2 h. Further increase in contact time does not change significantly dye removal. Fast adsorption at the initial contact time is due to the availability of surface sites. So, an agitation time of 2 h seems to be sufficiently long to achieve equilibrium.

Four kinetic equations including pseudo-first-order, pseudo-second-order, intraparticle diffusion and Elovich's models were tested to elucidate the adsorption mechanism. The parameters corresponding to employed models are reported in Table 3. The pseudo-first-order equation [16] was found suitable only for the initial 20 min of interaction (data not shown) and not fit for the whole range of contact time. The fit of the experimental data with the pseudo-second-order model is more appropriate. Linear plots of t/Q_t vs. t (Eq. (2)) [17] were obtained, corresponding to high R^2 values, i.e. >0.96. This model was also validated for RB5-activated carbon [28]. The initial sorption rate, h, increases with increasing adsorption temperature. For D800, the parameter h varies from 40.03 to 110.94 mg g^{-1} min^{-1}, when the temperature passes from 25 to 55 °C. Hence, the increase in temperature favors the initial adsorption process. The applicability of this equation indicates that the rate-limiting step may be chemisorption. Similar results have been reported for the RB5- biocomposite system [29].

When adsorption in batch mode is employed, the possibility of intraparticle pore diffusion of the adsorbate is always present. Weber and Morris [18] proposed that if the uptake of the adsorbate varies linearly with the square root of time, intraparticle diffusion can be taken as the rate-limiting step and if the plot passes through the origin, intraparticle diffusion will be the sole rate-limiting process. The plots of Q_t vs. $t^{1/2}$ (Eq. (4)) led to three linear portions (figures not shown). The first represents the external transport of mass, the second intraparticle diffusion and the last surface saturation [18]. The kinetic parameters of this model are gathered in Table 3. High determination coefficients (0.93–1.00), corresponding to the second

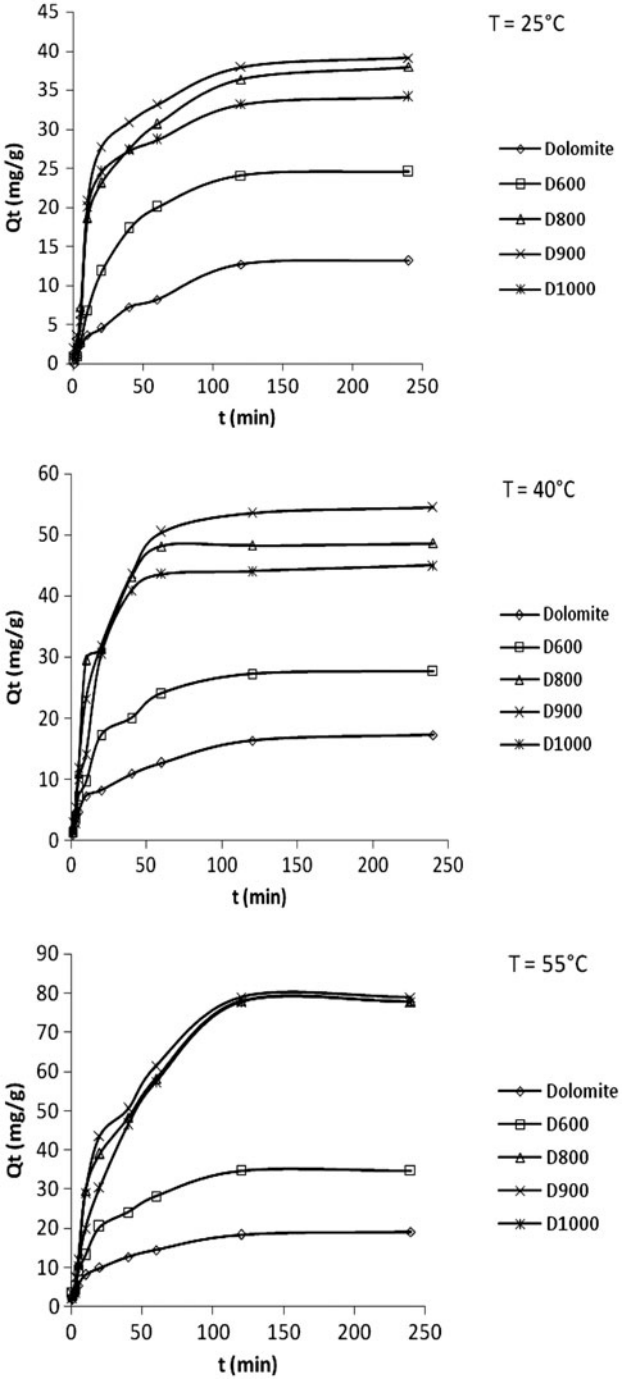

Fig. 3. Effect of contact time on the uptake of RB5 by the thermally treated dolomites at $C_{initial} = 80\ mg\ L^{-1}$.

linear portion, were obtained. The intraparticle diffusion rate constant, K_{id}, increases with temperature, indicating an enhancement of the pore diffusion into the dolomitic particles. The intraparticle diffusion cannot be accepted as the only rate-controlling step, due to the deviation of the plots from the origin (C values $\neq 0$). As consequence, the process becomes rather complex and involves more than one diffusive resistance, the boundary layer diffusion affecting the RB5 adsorption to some extent.

The Elovich equation is one of the most useful models for describing an activated chemisorption onto highly heterogeneous adsorbents. The coefficients of Elovich, α and β, are known to represent the initial adsorption rate and the desorption constant, respectively. These parameters were computed from the plots of Q_t vs. ln t (Eq. (5)) [19]. The obtained R^2 values (Table 3) confirm the applicability of this equation. The α values increase overall with temperature at the expense of those of β. As α represents the initial rate of adsorption, its increase might be associated with that of the diffusivity of the dye molecule, while the evolution of β would be explained by the difficulty of desorbing the molecules of RB5.

The kinetic mechanism is enough complex, involving different models. However, a close agreement exists between the evolution of values of h (pseudo-second-order), K_{id} (intraparticle diffusion), and α (Elovich), which increase with increasing adsorption temperature. This evolution implicitly indicates chemisorption, i.e. an increase in adsorption with increasing batch temperature, as found from Fig. 3.

3.3. Adsorption equilibrium

3.3.1. Isotherms

The equilibrium adsorption of RB5 onto dolomite, D600, D800, D900, and D1000 was studied via a bath process at 25, 40, and 55°C. The RB5 adsorption isotherms are depicted in Fig. 4. For all dolomitic solids, the adsorption capacity strongly increases with increasing temperature. At 25 and 55°C and a C_i value of $400\ mg\ L^{-1}$, D900 adsorbs 51.8 and $125.9\ mg\ g^{-1}$, respectively, so that RB5 molecules become more reactive at higher temperatures. This feature suggests that the adsorption mechanism involves a chemical process. Whatever temperature, the affinity follows the sequence D900 > D800 > D1000 > D600 > raw dolomite. The different adsorption capacities found for D, D600, D800, D900, and D1000 would be explained and correlated with their crystallographic properties and weight loss percentage (Table 2). The decomposition of dolomite ($CaCO_3.MgCO_3$) in MgO and CaO species, the presence of a certain content of calcite, and a weight loss of 47% would explain the highest capacity of D900. In return, the lowest capacity of raw dolomite could be due to a $CaCO_3.MgCO_3$ phase without decomposition and, thus, without CO_2 removal, for which there is no weight loss.

Table 3
Kinetic parameters of the RB5 adsorption by the thermally treated dolomites

			Pseudo-second-order model				Intraparticle diffusion model			Elovich's model			
Samples	T (°C)	Q_e (exp) (mg g^{-1})	Q_e (cal) (mg g^{-1})	K_2 (g mg^{-1} min^{-1})	h (mg g^{-1} min^{-1})	R^2	K_{id} (mg g^{-1} min$^{-1/2}$)	C (mg g^{-1})	R^2	Q_e (cal) (mg g^{-1})	α (mg g^{-1} min^{-1})	β (g mg^{-1})	R^2
Dolomite	25	12.72	14.92	0.0452	7.33	0.961	1.058	0.163	0.975	11.75	1.54	0.404	0.940
	40	16.36	18.86	0.0502	13.54	0.995	1.231	3.091	0.985	16.57	3.74	0.286	0.984
	55	18.40	20.40	0.0537	18.21	0.996	1.340	3.768	0.999	19.04	3.00	0.315	0.984
D600	25	24.09	26.06	0.0242	14.07	0.962	2.879	1.647	0.983	29.89	1.82	0.203	0.927
	40	27.27	28.37	0.0422	31.40	0.994	2.925	1.853	0.927	33.89	2.61	0.181	0.973
	55	34.77	34.98	0.0391	47.28	0.995	3.808	4.761	0.953	38.50	6.68	0.150	0.974
D800	25	36.36	43.47	0.0302	40.03	0.987	2.582	10.98	0.990	39.26	6.27	0.136	0.964
	40	48.27	55.55	0.0317	73.91	0.986	4.393	14.21	0.960	62.23	10.08	0.097	0.929
	55	77.95	90.90	0.0182	110.94	0.979	6.058	10.87	0.994	77.33	10.13	0.063	0.956
D900	25	37.95	43.47	0.0338	48.79	0.990	2.531	14.44	0.936	42.16	7.42	0.125	0.949
	40	53.63	62.50	0.0288	83.07	0.994	6.004	4.69	0.995	70.46	9.85	0.089	0.964
	55	78.95	90.90	0.0203	127.11	0.992	6.559	10.54	0.960	82.39	12.0	0.064	0.964
D1000	25	33.18	23.01	0.0335	36.95	0.975	0.763	22.78	0.927	31.13	7.20	0.143	0.918
	40	44.09	54.70	0.0271	52.76	0.968	8.192	10.10	0.950	54.19	7.85	0.103	0.929
	55	77.68	75.50	0.0146	88.11	0.971	8.294	5.943	0.999	80.81	9.50	0.065	0.939

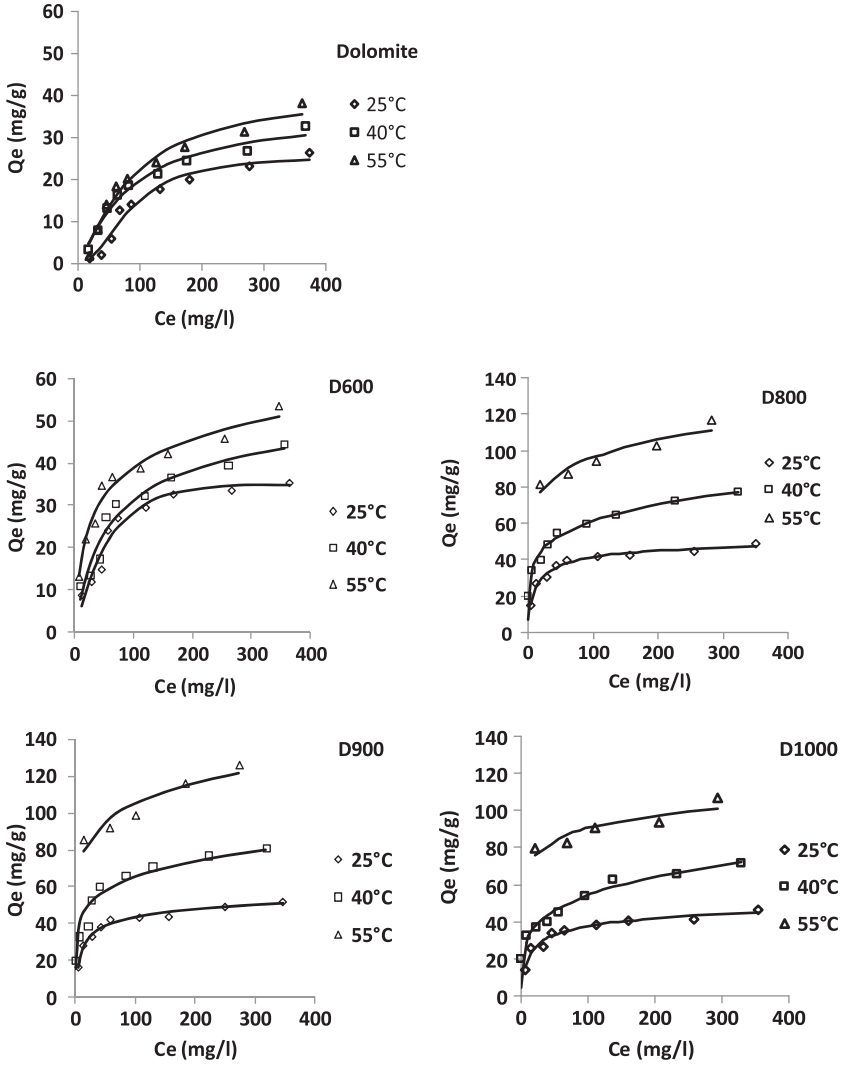

Fig. 4. Isotherms according to the RP model (—) and experimental data (…) for D600, D800, D900, and D1000. Isotherms according to the LF model (—) and experimental data (…) for dolomite.

At 55˚C, the maximum uptake capacity of D900 is 3.3 times higher than that of raw dolomite. This ratio falls to 1.97 at 25˚C, so that the temperature effect on the retention capacity is more accentuated for a calcined dolomite. Using the classification of Giles et al. [30], the isotherms of dolomite and D600 are L-shaped. The initial curvature of the L-curve shows that the contaminant has a high affinity for the surface, while the slope falls steadily with a rise in concentration. For D800, D900, and D1000, the increase in the adsorption temperature from 40 to 55˚C transforms the curves from L- to H-shape. The H-type isotherms are indicative of adsorbate–substrate chemical forces rather than physical attraction. Our H-curves may be conformed to the H3 subgroup [31]. Curves of H3-type represent systems in which the adsorbate monolayer has been completed. Probably, it is about a chemisorbed monolayer, on the basis of the discussion above. The completion of this first layer is accompanied by a short plateau for the isotherms of D800, D900, and D1000, at 55˚C. The subsequent rise represents the development of a second layer except that the latter is not complete and the forces generating it are weaker than those generating the first [31].

3.3.2. *Fitting the models to the experimental data*

Fitting of adsorption isotherm equations to experimental data is an important aspect of data analysis. The Langmuir [20] and Freundlich [21] models are widely used since they are simple and have an ability to describe experimental results in a wide range of

concentrations. The accuracy of the fit of a model with the experimental data is given by the determination coefficient, R^2, which is the square of the correlation coefficient, R, and the average relative error, $E\%$. The sample was eliminated on the basis of a determination coefficient lower than 0.90 and an average relative error higher than 20%. The linearization parameters of both Langmuir and Freundlich models are summarized in Table 4. Except for some particular cases, the Langmuir isotherm (Eq. (6)) shows an inadequate fit of the experimental data, giving E values as high as 96% (D1000 at 55°C). The very low representativeness of this model with respect to our experimental data can be explained from its hypotheses: an adsorbent where all sites are identical and energetically equivalent seems to be unlikely in the RB5 adsorption by dolomitic solids, as discussed above. The application of the Freundlich equation (Eq. (7)) to the isotherms of untreated dolomite is inappropriate. A relatively better description is obtained especially for D800, D900, and D1000; the average relative error values being lower than those of Langmuir. This feature indicates that adsorption takes place onto energetically heterogeneous solids. However, the obtained results are found to be contradictory: although the E values are interesting those of R^2 are somewhat low (D800, D900, and D1000). The restricted validity of this model by considering all samples also can be explained from its hypotheses: a physical process for RB5-dolomitic solid systems is improbable, at least at high temperature.

The LF [22] and RP [23] models were used for the mathematical description of the adsorption equilibrium. These isotherm equations include three adjustable parameters and require nonlinear least-squares (NLLS) analysis. The related parameters were calculated and tabulated in Table 5. The isotherms of RP (Eq. (9)) describe efficiently the RB5 adsorption onto D600, D800, D900, and D1000 (Fig. 4); the E values are globally <10% with $R^2 > 0.90$. On the contrary, a poor agreement is found with dolomite. This model was found to be appropriate for the adsorption of RB5 onto activated carbons [32]. The K_{RP} values increase with the adsorption temperature and, at 55°C, decrease in the order D900 > D800 > D1000 >> D600, i.e. according to the affinity sequence. For D800, D900, and D1000, the β exponent lies between 0 and 1, indicating a favorable adsorption onto heterogeneous adsorbents. The surface heterogeneity factor β, depends on the surface properties, degree of crystallinity, and distribution of active adsorption centers. Stefaniak et al. [33] found that many reasons are responsible for the energetic heterogeneity of the surfaces of dolomitic materials, namely the presence of Ca and Mg ions in the surface structure, the chemistry

Table 4
Adjustable parameters estimated from linear regression

			Langmuir model				Freundlich model			
Samples	T (°C)	Q_{exp} (mg g^{-1})	Q_m (mg g^{-1})	K_L (L mg^{-1})	R^2	E (%)	K_F (L mg^{-1})$^{1/n}$	n	R^2	E (%)
Dolomite	25	26.4	333.3	0.0003	0.008	33.97	0.08	0.95	0.854	35.85
	40	32.7	45.4	0.0069	0.935	11.16	0.82	1.52	0.885	19.06
	55	38.2	76.9	0.0030	0.322	29.34	0.66	1.19	0.797	36.38
D600	25	35.4	41.7	0.0188	0.985	11.14	3.23	2.28	0.885	0.90
	40	44.4	52.6	0.0165	0.981	13.60	4.27	2.42	0.911	0.28
	55	53.6	55.6	0.0293	0.986	10.13	8.20	3.03	0.937	49.57
D800	25	49.1	50.0	0.0597	0.995	07.54	12.67	4.08	0.883	10.24
	40	77.3	83.3	0.0558	0.991	0.19	29.19	6.49	0.956	1.01
	55	116.8	125.0	0.1428	0.989	45.86	47.61	6.13	0.813	17.47
D900	25	51.8	52.6	0.0603	0.995	15.73	9.57	2.75	0.738	19.79
	40	80.9	83.3	0.0666	0.995	42.09	4.35	6.02	0.917	10.86
	55	125.9	125.0	0.1530	0.989	42.97	51.64	6.13	0.859	16.27
D1000	25	46.3	47.6	0.0484	0.994	9.35	11.14	3.39	0.888	9.41
	40	71.8	76.9	0.0424	0.989	23.83	27.30	6.99	0.903	11.33
	55	106.8	111.1	0.0004	0.991	96.07	45.83	6.41	0.748	18.76

Table 5
Adjustable parameters estimated from NLLS method

			Langmuir-Freundlich model					Redlich-Peterson model				
Samples	T (℃)	Q_{exp} (mg g^{-1})	K_{LF} (L g^{-1})	β	a_{LF} (L mg^{-1})$^{\beta}$	R^2	E (%)	K_{RP} (L g^{-1})	β	a_{RP} (L mg^{-1})$^{\beta}$	R^2	E (%)
Dolomite	25	26.4	0.003	2.081	9.71×10^{-5}	0.969	20.16	0.156	1.691	5.72×10^{-5}	0.951	44.72
	40	32.7	0.206	1.166	0.0057	0.977	10.54	0.375	0.997	0.010	0.976	12.98
	55	38.2	0.136	1.280	0.0033	0.970	25.37	0.365	1.040	0.005	0.967	32.25
D600	25	35.4	0.320	1.255	0.0083	0.948	11.39	0.010	1.227	0.004	0.952	10.71
	40	44.4	1.547	0.832	0.0278	0.945	11.77	0.024	0.922	0.033	0.944	12.31
	55	53.6	5.223	0.635	0.0785	0.966	5.66	0.126	0.841	0.176	0.970	4.98
D800	25	49.1	7.046	0.748	0.1373	0.976	4.39	0.156	0.927	0.180	0.979	3.96
	40	77.3	26.370	0.205	0.0435	0.972	6.73	25.650	0.801	13.440	0.962	9.31
	55	116.8	83.110	0.128	0.2909	0.757	6.59	619.70	0.865	260.15	0.892	4.11
D900	25	51.8	9.524	0.661	0.1693	0.979	3.75	0.227	0.906	0.261	0.984	2.99
	40	80.9	49.520	0.384	0.5899	0.803	17.77	285.10	0.825	106.01	0.930	10.83
	55	125.9	58.480	0.172	0.1045	0.881	4.98	633.40	0.855	248.56	0.901	4.78
D1000	25	46.3	7.336	0.638	0.1410	0.957	5.93	0.187	0.892	0.224	0.962	5.37
	40	71.8	22.502	0.211	0.0334	0.929	10.40	23.320	0.761	10.980	0.940	10.90
	55	106.8	64.661	0.140	0.1879	0.815	4.15	446.30	0.894	233.33	0.902	4.06

of adsorption sites, crystallographic defects, the influence of neighboring sites, impurities of surface, etc. As a complement of the RP model, that of LF (Eq. (8)) Table 5 provides a satisfactory description of the dolomite isotherms (Fig. 4). The β_{LF} values for dolomite are >1, which is the sign of an unfavorable adsorption onto an energetically homogeneous material.

3.4. Thermodynamic parameters

The values of free energy (ΔG), enthalpy (ΔH), and entropy (ΔS) are presented in Table 6. The obtained results are reliable because the determination coefficients are suitable. The ΔG values are positive in the temperature range studied, revealing that the process is not spontaneous with a possibility of chemisorption. The calculated free energies are found to decrease with temperature, which indicates that better adsorption is obtained at high temperature. The lowest value manifested by D900 at 55℃ confirms its highest adsorption capacity. The positive ΔH values indicate that the RB5 adsorption is endothermic. Thereby, the process is favored by an increase in temperature through the activation of the adsorption sites. The positive values of ΔS suggest an increase in randomness at the solid–solution interface and significant changes occur in the internal structure of the adsorbents, once the adsorptive is retained [34].

Table 6
Thermodynamic parameters for the RB5 adsorption onto thermally treated dolomites

Samples	ΔH (kJ mol^{-1})	ΔS (J mol^{-1} K^{-1})	ΔG (kJ mol^{-1})			R^2
			25℃	40℃	55℃	
Dolomite	10.07	15.62	5.41	5.18	4.95	0.987
D600	8.51	14.93	4.06	3.83	3.61	0.993
D800	32.05	96.51	3.29	1.84	0.40	0.995
D900	33.87	103.08	3.15	1.61	0.058	0.999
D1000	31.97	95.76	3.43	1.99	0.56	0.999

3.5. Influence of pH

The effect of initial pH is illustrated in Fig. 5 at $C_{initial} = 80$ mg L^{-1}; the purpose being to study pH influence on the adsorption of RB5 under similar conditions. The shape of the curves is not identical for all minerals. Strong pH-dependence exists for D800, D900, and D1000, contrary to raw dolomite and D600, for which this dependence is moderate. The retention of RB5 is found to increase up to 6–7, beyond which it decreases. For illustration, the capacity of D900 at pH 3, 7, and 11 is 5, 40.5 and 30.2 mg g^{-1}, respectively. Reactive dyes are known to ionize to a high degree in

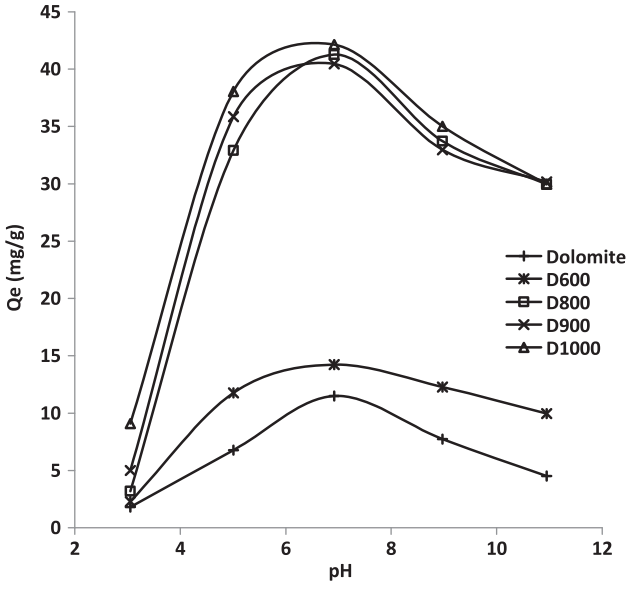

Fig. 5. Adsorption of RB5 by the thermally treated dolomites as a function of pH at $C_{initial} = 80\ mg\ L^{-1}$.

aqueous media to form colored anions, due to the presence of sulfonate group(s) in their structures. The latter dissociate so that the dye becomes anionic. The decrease in the RB5 adsorption at higher pH values could be due to the formation of OH^- ions which compete with the dye anionic species for the occupancy of adsorption sites. In a previous paper [35], an isoelectric point of 6.8 (pH_{iep}) was found. It must be expected that for $pH < pH_{iep}$, the retention ability increases with decreasing initial pH of the solution, consequence to the electrostatic attraction between the dye molecules (negatively charged) and positively charged adsorption sites [25]. Since such an evolution is not true, the RB5 adsorption by dolomitic solids is not primarily controlled by electrostatic forces involving the sulfonate groups [36]. Such dependence would result in higher adsorption at lower pH.

According to the nature of material, reactive dyes are capable of interacting with its surface via several mechanisms such as coulombic and hydrophobic–hydrophobic interactions, hydrogen bonding, and surface complexation. We cannot imply hydrogen bonding since the RB5 adsorption onto the calcined derivatives of dolomite is much more reactive at 55°C than 25 and 40°C, as mentioned above from isotherm data. From temperature-dependent FTIR experiments, it was found a disturbing and weakening of H-bonds with increasing temperature [37]. Hydrophobic–hydrophobic interactions also appear unlikely because dolomitic surfaces do not have the characteristics of hydrophobicity. The interactive process seems somewhat difficult to explain. Its complexity would be explained by the nature of the dye and the adsorbent. RB5 is a reactive azo-dye containing different types of functional groups such as $–NH_2$, –S=O, –O–H, while dolomitic solids are prone to a complex surface speciation, due to the presence of dolomite, calcite, periclase, and lime, according to treatment temperature as mentioned above. The fact that maximum adsorption occurs at isoelectric point highlights the prevalence of the nonelectrostatic interaction. The latter is indicative of a weak chemical interaction [38] between the surfaces of dolomitic solids and the functional groups of RB5. A weak chemical interaction could consist of complexation-type bond [39]. From FTIR and XPS analyses, Hou et al. [40] showed that the mechanism of the Congo red (sulfonated diazo dye as RB5) adsorption by Ca^{2+} in hydroxyapatite/chitosan composite, involved surface complexation. RB5 possesses two different donor atoms: N (of amino or azo groups) and O (of sulfonate groups). These donor atoms may be involved in the complexation of RB5 at the surface of dolomitic solids.

3.6. FTIR analysis

FTIR spectroscopy technique was used to elucidate the adsorption mechanism. The properties of dolomite in the infrared region have been summarized by White [41]. The infrared spectra of D900 and RB5, before and after adsorption (RB5-loaded D900), were recorded in the 4,000–400 cm^{-1} range (Fig. 6). As seen from this figure, the band at 450 cm^{-1} could be correlated with the vibration of the Mg–O bond (Fig. 6–D900). There are two strong bands in the mid-infrared region, which are due to the internal modes of the CO_3^{2-} ion and assigned to two infrared active fundamental vibrations: ν_2 out-of-plane bending and ν_3 asymmetric stretching at 875 and 1,439 cm^{-1}, respectively. The latter vibration shows a very broad band which results from large splitting of the transverse and longitudinal components of the vibration [42]. When a calcined dolomitic solid is again exposed to air, i.e. to a minor amount of CO_2 and H_2O vapors, several spectral characteristics that were eliminated by decarbonation, consequence of the thermal treatment, are restored [43]. On this basis, the bands at 1,439 and 875 cm^{-1} are due to CO_2 recovered. The presence of the bands at 3,703, 3,660, and 3,447 cm^{-1} could be caused by a hydroxyl (OH) associated with a metastable hydroxylated magnesium oxide structure [43]. The formation of magnesium oxide is the consequence of the Eq. (13). The frequency at 2,685 cm^{-1} was ascribed to hydroxylated CaO [44]. The

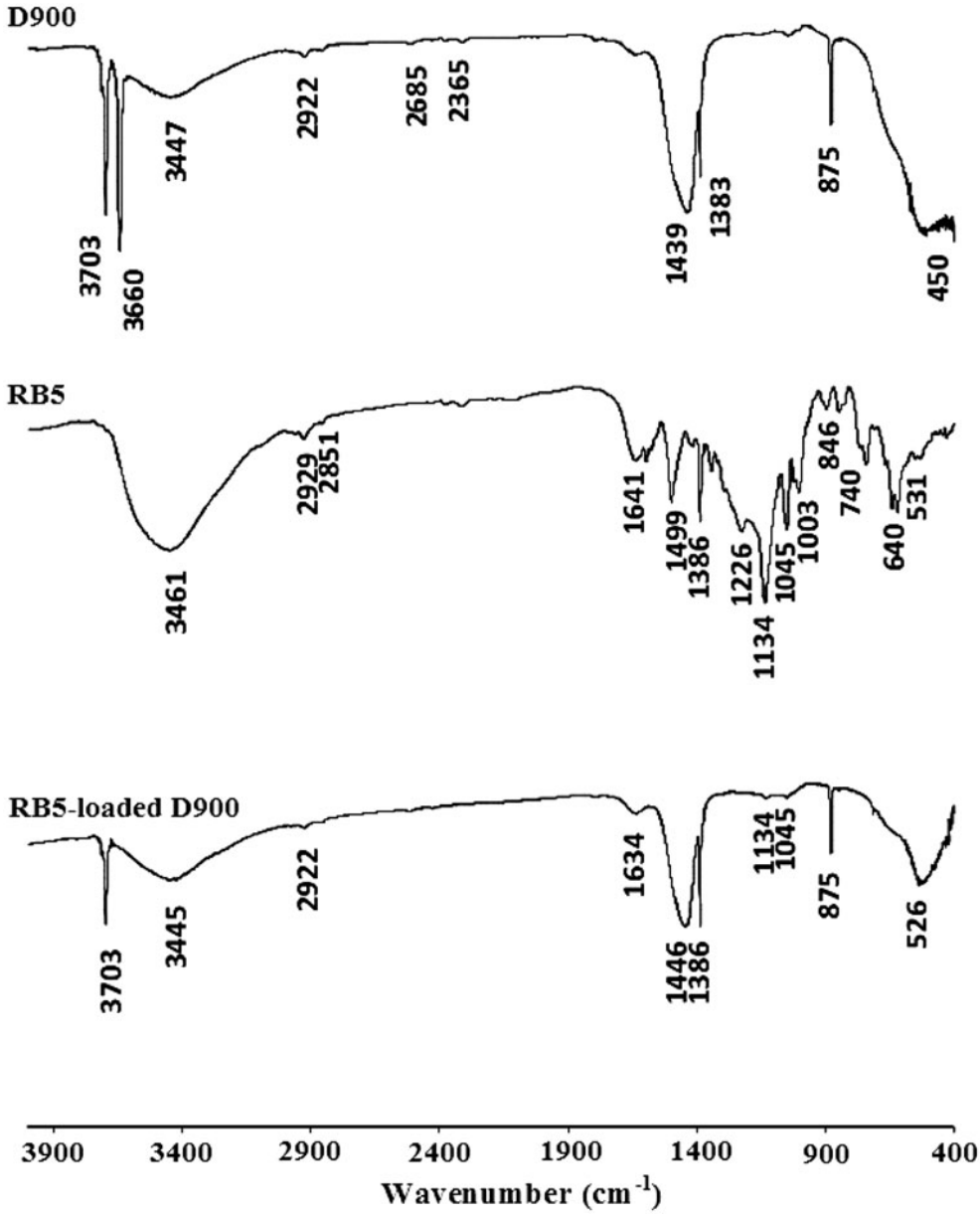

Fig. 6. FTIR spectra of D900, RB5, and RB5-loaded D900.

bands observed at 2,922 and 2,365 cm^{-1} prove the presence of calcite and quartz, respectively. These observations agree with those resulting from XRD and SEM analyses.

The FTIR spectrum of RB5 before adsorption (Fig. 6–RB5) exhibits a broad band in the 3,700–3,000 cm^{-1} range, which may be due to the overlapping of N–H and O–H stretching vibrations. The peak at 2,929 cm^{-1} and the shoulder at 2,851 cm^{-1} are assigned to asymmetric and symmetric CH_2 groups, respectively. Ones at 1,641 and 1,499 cm^{-1} are indicative of the skeletal vibrations of the aromatic ring, through C=C bond. The medium band appearing at 1,226 cm^{-1} may be linked to the amino C–N stretching. The peaks at 1,386 and 1,134 cm^{-1} characterize the asymmetric and symmetric vibrations of sulfone groups (SO_2), while that at 1,045 cm^{-1} is the consequence of the S=O stretching. The 1,003 cm^{-1} band represents the stretch of the S–O–C species. The interval 900–650 cm^{-1} contains many bands related to the aromatic out-of-plane C–H bending. The frequency near 531 cm^{-1} belongs to the N–H twisting mode. The assignment of the RB5

bands was carried out from the book of Silverstein et al. [45].

Fig. 6 (RB5−loaded D900) displays the results of D900 after exposure to a solution of 400 mg L^{-1} of RB5, at pH 6.9. The spectrum of the RB5-loaded D900 highlights a certain number of alterations of the absorption bands: some vanish while others are found to shift. These spectral features confirm the complexation of the RB5 molecule on the surface of D900, through its functional groups. The strong and broad bands at 3,445 and 526 cm^{-1} denote a deep involvement of amino groups in the complexation of magnesium oxide, on the basis of the discussion above and from Eq. (13), forming thereby inner-sphere surface complexes. The latter are created as a result of the weak chemical bond formation between anionic species (Lewis base) and the metallic ions at the solid surface (Lewis acid), and nitrogen atoms providing nonbonding electrons to establish this bond. This form of surface complexation is intermediate in strength between ionic and covalent bonds. The bands at 1,134 and 1,045 cm^{-1} disappear almost completely, suggesting that the sulfone (SO_2) and sulfoxide (S=O) groups are involved in the RB5 adsorption. This behavior would indicate that an outer-sphere surface complexation also takes place via the oxygen atoms of SO and SO_2.

4. Conclusion

The heating of dolomite at 600˚C for 2 h does not modify the structure significantly. On the contrary, the products calcined at 800 and 900˚C partially decompose, leading to rigid porous calcite and fine powdered magnesium oxide. Dolomite treated at 1,000˚C undergoes a total decomposition with the formation of an oxide crystal network constituted of lime and periclase. From 800˚C, the SEM images evidence a more porous structure with newly created pores and slots so that the adsorption of RB5 by D800, D900, and D1000 is favored.

A close agreement exists between the evolution of kinetic, equilibrium, and thermodynamic parameters, suggesting chemisorption, while maximum adsorption occurs at isoelectric point. The process reflects for D800, D900, and D1000, mainly, a weak chemical interaction via a mechanism of inner-sphere complexation. The latter intervenes between nonbonding electrons of nitrogen atoms associated with amino groups and the surface oxides: MgO and/or CaO according to treatment temperature.

The affinity of the dolomitic solids for RB5 is D900 > D800 > D1000 > D600 > raw dolomite. Knowing that D900 adsorbs 125.9 mg g^{-1}, it has the potential to act as an adsorbent for the removal of reactive dyes from wastewaters.

References

[1] R. Gong, X. Zhang, H. Liu, Y. Sun, B. Liu, Uptake of cationic dyes from aqueous solution by biosorption onto granula kohlrabi peel, Bioresour. Technol. 98 (2007) 1391–1423.
[2] T.O. Mahony, E. Guibal, J.M. Tobin, Reactive dye biosorption by *Rhizopus arrhizus* biomass, Enzyme Microb. Technol. 31 (2002) 456–463.
[3] Y.S. Al-Degs, M.I. El-Barghouthi, A.H. El-Sheikh, G.A. Walker, Effect of solution pH, ionic strength, and temperature on adsorption behavior of reactive dyes on activated carbon, Dyes Pigm. 77 (2008) 16–23.
[4] G. Crini, Non-conventional low-cost adsorbents for dye removal: A review, Bioresour. Technol. 97 (2006) 1061–1085.
[5] M. Asgher, Biosorption of reactive dyes: A review, Water Air Soil Pollut. 223 (2012) 2417–2435.
[6] B. Kokabian, B. Bonakdarpour, S. Fazel, The effect of salt on the performance and characteristics of a combined anaerobic–aerobic biological process for the treatment of synthetic wastewaters containing reactive black 5, Chem. Eng. J. 221 (2013) 363–372.
[7] S.A. Ong, L.N. Ho, Y.S. Wong, S.F. Chen, M. Viswanathan, R. Bahari, Mineralization of diazo dye (reactive black 5) in wastewater using recirculated up-flow constructed wetland reactor, Desalin. Water Treat. 46 (2012) 312–320.
[8] S.K. Sharma, H. Bhunia, P.K. Bajpai, Photocatalytic decolorization kinetics and adsorption isotherms of a mixture of two anionic azo dyes: Reactive red 120 and reactive black 5, Desalin. Water Treat. 44 (2012) 261–268.
[9] A. Nora'aini, A. Norhidayah, A. Jusoh, The role of reaction time in organic phase on the preparation of thin-film composite nanofiltration (TFC-NF) membrane for dye removal, Desalin. Water Treat. 10 (2009) 181–191.
[10] M. Rabah, E.M.M. Ewais, Multi-impregnating pitch-bonded Egyptian dolomite refractory brick for application in ladle furnaces, Ceram. Int. 35 (2009) 813–819.
[11] O. Ilgen, Dolomite as a heterogeneous catalyst for transesterification of canola oil, Fuel Process. Technol. 92 (2011) 452–455.
[12] F. Tamaddon, M. Tayefi, E. Hosseini, E. Zare, Dolomite ($CaMg(CO_3)_2$) as a recyclable natural catalyst in Henry, Knoevenagel, and Michael reactions, J. Mol. Catal. A: Chem. 366 (2013) 36–42.
[13] K. Marouf-Khelifa, A. Khelifa, A. Belhakem, R. Marouf, F. Abdelmalek, The adsorption of pentachlorophenol from aqueous solutions onto exchanged Al-MCM-41materials, Adsorpt. Sci. Technol. 22 (2004) 1–12.
[14] S. Kadi, S. Lellou, K. Marouf-Khelifa, J. Schott, I. Gener-Batonneau, A. Khelifa, Preparation, characterisation and application of thermally treated Algerian halloysite, Micropor. Mesopor. Mater. 158 (2012) 47–54.

[15] K. Belkassa, F. Bessaha, K. Marouf-Khelifa, I. Batonneau-Gener, J.D. Comparot, A. Khelifa, Physicochemical and adsorptive properties of a heat-treated and acid-leached Algerian halloysite, Colloids Surf., A 421 (2013) 26–33.
[16] S. Lagergren, Zur theorie der sogenannten adsorption gelöster stoffe, Zur theorie der sogenannten adsorption gelöster stoffe, Kungliga Svenska Vetenskapsademiens (About the theory of so-called adsorption of soluble substances, K. Sven. Vetenskapsakad), Handl. 24 (1898) 1–39.
[17] Y.S. Ho, G. McKay, Pseudo-second order model for sorption process, Process Biochem. 34 (1999) 451–465.
[18] W.J. Weber, J.C. Morris, Kinetics of adsorption on carbon from solution, J. Sanitary Eng. Div. Am. Soc. Civ. Eng. 89 (1963) 31–59.
[19] S.H. Chien, W.R. Clayton, Application of Elovich equation to the kinetics of phosphate release and sorption in soils, Soil Sci. Soc. Am. J. 44 (1980) 265–268.
[20] I. Langmuir, Adsorption of gases on plane surfaces of glass, mica and platinum, J. Am. Chem. Soc. 40 (1918) 1361–1403.
[21] H.M.F. Freundlich, Over the adsorption in solution, J. Phys. Chem. 57 (1906) 385–470.
[22] M. Jaroniec, A. Derylo, A.W. Marczewski, The Langmuir–Freundlich equation in adsorption from dilute solutions on solids, Monatsh. Chem. 114 (1983) 393–397.
[23] O. Redlich, D.L. Peterson, A useful adsorption isotherm, J. Phys. Chem. 63 (1959) 1024–1033.
[24] R. Marouf, N. Khelifa, K. Marouf-Khelifa, J. Schott, A. Khelifa, Removal of pentachlorophenol from aqueous solutions by dolomitic sorbents, J. Colloid Interface Sci. 297 (2006) 45–53.
[25] F. Boucif, K. Marouf-Khelifa, I. Batonneau-Gener, J. Schott, A. Khelifa, Preparation, characterisation of thermally treated Algerian dolomite powders and application to azo-dye adsorption, Powder Technol. 201 (2010) 277–282.
[26] H.G. Wiedemann, G. Bayer, Note on the thermal decomposition of dolomite, Thermochim. Acta 121 (1987) 479–485.
[27] S. Karaca, A. Gürses, M. Ejder, M. Açikyildiz, Adsorptive removal of phosphate from aqueous solutions using raw and calcinated dolomite, J. Hazard. Mater. 128 (2006) 273–279.
[28] A.A. Ahmad, A. Idris, B.H. Hameed, Organic dye adsorption on activated carbon derived from solid waste, Desalin. Water Treat. 51 (2013) 2554–2563.
[29] C. Umpuch, S. Sakaew, Adsorption characteristics of reactive black 5 onto chitosan- intercalated montmorillonite, Desalin. Water Treat. doi: 10.1080/19443994.2013.867541.
[30] C.H. Giles, T.H. Mc Ewan, S.N. Nakhwa, D. Smith, Studies in adsorption. Part XI. A system of classification of solution adsorption isotherms, and its use in diagnosis of adsorption mechanisms and in measurement of specific surface areas of solids, J. Chem. Soc. 60 (1960) 3973–3993.
[31] C.H. Giles, D. Smith, A. Huitson, A general treatment and classification of the solute adsorption isotherm: I. Theoretical, J. Colloid Interface Sci. 47 (1974) 755–765.
[32] A.W.M. Ip, J.P. Barford, G. McKay, A comparative study on the kinetics and mechanisms of removal of Reactive Black 5 by adsorption onto activated carbons and bone char, Chem. Eng. J. 157 (2010) 434–442.
[33] E. Stefaniak, B. Bilinski, R. Dobrowolski, P. Staszczuk, J. Wojcik, The influence of preparation conditions on adsorption properties and porosity of dolomite-based sorbents, Colloids Surf., A 208 (2002) 337–345.
[34] M. Alkan, Ö. Demirbaş, M. Doğan, Adsorption kinetics and thermodynamics of an anionic dye onto sepiolite, Microporous Mesoporous Mater. 101 (2007) 388–396.
[35] R. Marouf, K. Marouf-Khelifa, J. Schott, A. Khelifa, Zeta potential study of thermally treated dolomite samples in electrolyte solutions, Microporous Mesoporous Mater. 122 (2009) 99–104.
[36] E. Fu, P. Somasundaran, Alizarin Red S as a flotation modifying agent in calcite–apatite systems, Int. J. Miner. Process 18 (1986) 287–296.
[37] K.J. Eichhorn, A. Fahmi, G. Adam, M. Stamm, Temperature-dependent FTIR spectroscopic studies of hydrogen bonding of the copolymer poly(styrene-b-4-vinylpyridine) with pentadecylphenol, J. Mol. Struct. 661–662 (2003) 161–170.
[38] D.S. Cicerone, A.E. Regazzoni, M.A. Blesa, Electrokinetic properties of the calcite/water interface in the presence of magnesium and organic matter, J. Colloid Interface Sci. 154 (1992) 423–433.
[39] R.T. Yang, Adsorbents: Fundamentals and Applications, Wiley, New Jersey, NJ, 2003.
[40] H. Hou, R. Zhou, P. Wu, L. Wu, Removal of congo red dye from aqueous solution with hydroxyapatite/chitosan composite, Chem. Eng. J. 211–212 (2012) 336–342.
[41] W.B. White, The carbonate minerals, in: V.C. Farmer (Ed.), The Infrared Spectra of Minerals, Mineralogical Society Monograph 4, The Mineralogical Society, London, 1974, pp. 227–284.
[42] O.S. Pokrovsky, J.A. Mielczarski, O. Barres, J. Schott, Surface speciation models of calcite and dolomite/aqueous solution interfaces and their spectroscopic evaluation, Langmuir 16 (2000) 2677–2688.
[43] J. Ji, Y. Ge, W. Balsam, J.E. Damuth, J. Chen, Rapid identification of dolomite using a Fourier transform infrared spectrophotometer (FTIR): A fast method for identifying Heinrich events in IODP Site U1308, Mar. Geol. 258 (2009) 60–68.
[44] H. Jacobs, M.J.D. Low, Infrared spectroscopic study of the thermal decomposition of dolomite in vacuum, J. Colloid Interface Sci. 46 (1974) 165–176.
[45] R.M. Silverstein, G.C. Bassler, T.C. Morrill, Spectrometric Identification of the Organic Compounds, fifth ed., De Boeck Université, Bruxelles, 1998. (in French).